Numerical Analysis of Absorber Layer, Thickness, Bandgap, Temperature, and Interface Defect Density of Perovskite Solar Cells by Device Simulation

Abstract

The numerical analysis was performed on lead-based perovskite solar cells (PSCs) to enhance the cell's performance, minimize toxicity, and improve cell stability. The solar cell capacitance simulator (SCAPS-1D) was used to investigate the effect of the thickness, bandgap, temperature, and interface defect density of the PSC. The SCAPS-1D consists of several layers; during the simulation, the Cu_2O was used as the hole transport layer (HTL), the TiO_2 was utilized as the electron transport layer (ETL), and the methylammonium lead triiodide ($MAPbI_3$) was used as the absorber layer. A fluorine-doped tin oxide (FTO) was deployed to perform the function of a front contact and transparent conductive oxide. The platinium serves as the back metal contact and also a means to minimize toxicity in lead. The variation in the thickness of the absorber layer recorded the highest PCE of 28.46% as the thickness increases to 1.0 μm but decrease at further increases in thickness. The device performance at lower interface defect density was higher and decreased as the defect density increased. The behaviour of the bandgap was also examined in the (ETL) and the results show the decrease in the PCE with increasing bandgap but on the contrary that of (HTL) increase in the PCE with increase in the bandgap. The PCE in the absorber layer also increases as the bandgap increases. The device's best operation temperature was between 280k and 340k.

Keywords: Simulation; Perovskite; Thickness; Bandgap; interface defect density; temperature

Introduction

In the ongoing evolution of solar cell technology, various materials and technologies have been explored to enhance efficiency and affordability. Several research works have concluded that; lead-based perovskite solar cells (PSCs) can emerge as groundbreaking and promising alternatives to traditional silicon-based solar cells [1,2,3]. PSCs have captured the attention of researchers worldwide due to their exceptional performance, ease of production, and potential for cost-effective mass manufacturing.

Nevertheless, like any technology, perovskites have their shortcomings that require mitigation for widespread development. The primary concern with perovskites is their environmental stability, as temperature instability compromises the stable solar cell operation [4, 5]. For instance, perovskite layers can delaminate at temperatures as low as 85°C in ambient conditions [6]. Many researchers have opined that, fast degradation of $MAPbI_3$ occurs at above 100°C and it is concerning that $MAPbI_3$ can slowly decompose to PbI_2 at elevated temperatures, even under an inert atmosphere like argon [7, 8]. Furthermore, the charge collection efficiency of the TiO_2 electron transport layer deteriorates over 5 hours when tested under ambient conditions with 1 sun illumination and an A.M spectrum, attributed to trapped electrons in unoccupied states [9].

There are however some deliberate efforts made by many researchers in order to overcome these shortcomings posed by PSCs. Notable among are the modification by the chemical composition of the perovskite materials, the coating of the perovskite layer with a passivation layer (such as metal oxides or organic materials), and encapsulating the cell with a protective layer that can reduce the impact of environmental factors on the stability of the cell and extend its lifetime [10, 11, 12, 13]. In 2022, Ni et al [14] uncovered where degradation occurs and the underlying mechanisms and defects involved in the performance degradation of P -I -N perovskite solar cells under illumination or reverse bias. They opined that light-induced degradation starts with the generation of iodine interstitials at the interface region between the perovskite and both charge transport layers. They also observed that trap annihilation of two types of iodine effects at the anode side, with negatively charged iodide interstitials near the cathode side that can be more detrimental to the solar cell efficiency. And concluded that, introducing a hole-blocking layer between the layers suppresses this interaction leading to an improvement in the reverse-bias stability.

In light of these challenges, this work also seeks to enhance the performance, power conversion efficiency, and stability of the PSCs by investigating the impact of key photovoltaic parameters, such as the thickness, the bandgap, the interface the defect density, and the temperature of PSCs using SCAPS ID simulator. We will also use platinum (Pt) as a back contact metal and this is because platinum is the least reactive metal to oxygen and moisture. This study holds significant promise for advancing perovskite solar cell technology, with its innovative model, comprehensive analysis of lead-based PSCs, and potential as a foundational resource for future research and outdoor testing. It aligns with the broader objective of developing more efficient and sustainable solar energy solutions.

.

SCAPS 1-D Numerical Simulation

Simulation can show the physical operation, the viability of the proposed physical model, and is an important way of understanding the device's operation. The device parameters instantly affect the physical operation and performance of the solar cell devices without the need to wait for long or spend money before seeing a result. The following simulation models have been used by several researchers in the photovoltaics technology COMSOL, SILVACO, TAD, SCAPS and MULTIPHYSICS [15, 16, 17, 18, 19]

In this work, Solar Cell Capacitance Simulator (SCAPS-1D) simulator is used to model the perovskite-based solar cells. The SCAPS 1D can be used to simulate PSC because it has a very intuitive operation window diversified models for grading, defects, recombination and generation. Though SCAPS has the ability to simulate only in 1D but it has other advantages like, it been user friendly, simulate under the dark and under illumination conditions. All simulations are carried out under global illumination of AM 1.5 spectrum with incident power density of $100\,\frac{mW}{cm^2}$ [20, 21] and the work function of the back contact metal is $5.65eV$.

The solar cell parameters can be obtained by solving the fundamental equations that dictate the charge transport in semiconductors listed as follows;

Poisson equations.

$$\frac{dE}{dx} = \frac{d^2\psi}{dx^2} = \frac{q}{e}[p(x) - n(x) + N_D^+(x) - N_A^-(x) + p_1(x) - n_1(x)] \quad (1)$$

Where $E$is the electric field, $\psi$is the electrostatic potential, $q$is the electorn charge, $e$is the dielectric constant of the semiconductor material, $p(n)$ is the hole (electron) concentration $N_A^-(N_D^+)$ is the density of the ionized acceptors (donors), $n_1(p_1)$ is the trapped electron (hole) and is the position coordinates.

The continuity equations of holes and electrons are;

$$\frac{dp_n}{dt} = G_p - \frac{p_n - p_{n_0}}{\Gamma_p} + p_n\mu_p\frac{dE}{dx} + \mu_p E\frac{dp_n}{dx} + D_p\frac{d^2p_n}{dx^2} \quad (2)$$

$$\frac{dn_p}{dt} = G_n - \frac{n_p - n_{p_0}}{\Gamma_n} + n_p\mu_n\frac{dE}{dx} + \mu_n E\frac{dn_p}{dx} + D_n\frac{d^2n_p}{dx^2} \quad (3)$$

Where G_n and G_p are the electron and hole generation rates D_n and D_p are the electron and hole diffusion coefficients.

This carrier transport occurs by the diffusion and the drift is expressed as follows;

$$J_n(x) = q_n\mu_n E + qD_n\frac{d_n}{dx} = n\mu_n\frac{dE_{f_n}}{dx} \quad (4)$$

$$J_p(x) = qp\mu_p E - qD_p\frac{dp}{dx} = p\mu_p\frac{dE_{f_p}}{dx} \quad (5)$$

Where μ_p and μ_n are the hole and electron mobilities respectively, and $E_{f_n}$and $E_{f_p}$are the quasi-fermi levels for electrons and holes.

Device Architecture and Methodology

The theoretical framework of the architectural model presents two different comparative models, based on lead-based hybrid perovskite material. In this study, the numerical analysis of lead-based perovskite solar cell will be optimized base on the existence experimental data in order to improve on the efficiency and tackle the problem of instability of the lead-based perovskite solar cell.

In this work, the device structure the initial and proposed cells for the simulation is carried out in n-i-p configuration of FTO/TiO_2/MAPbI3/CU_2O/pt as illustrated in Figure 1 (a) and (b). Here, Titanium oxide

(TiO_2) has be used as an electron transport layer (ETL) and Cuprous oxide (CU_2O) has been incorporated as hole transport layer (HTL). The lead-based perovskite (MAPbI3) is used as main absorber layer, which is sandwiched between ETL and HTL of both layers. Fluorine doped Tin Oxide (FTO) performs a dual function of serving as a front contact and as well as Transparent Conductive Oxide (TCO) through which light enters or passes. Platinium (Pt) acts as a back metal contact and also serve as a means to reduce the toxicity of lead.

The basic material information such as, bandgap of the materials, thickness of various layers, dopping concentration, mobility of electrons and holes, thermal velocities, electron affinity, dielectric permittivity, conduction band (CB) and Valence band (VB) effective density of states are required for simulation work which are also shown in Table 1 and the optimized parameters are shown in Table 2.

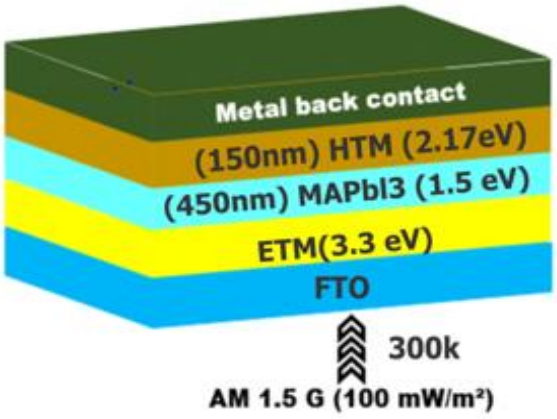

Figure (**a**)

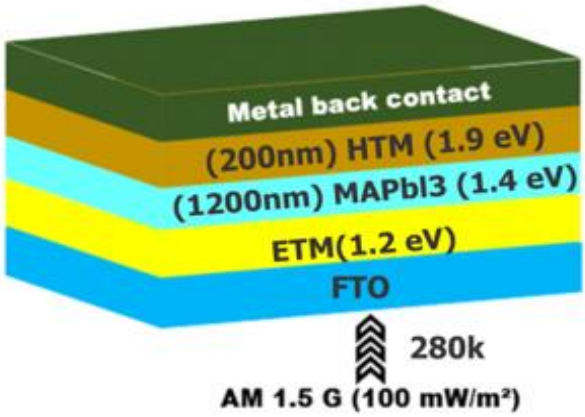

Figure (**b)**

Figure 1 (a): Device structure of lead-based PSC for the initial cell and Figure 1(b) is the proposed (optimized) cell.

Photovoltaic Parameters for the Simulation of PSCs Devices

Table1. Simulation Parameters adopted from [22, 23]

Parameters	FTO(SnO_2)	TiO_2 (ETL)	MAPbI3	CU_2O (HTL)
Thickness (nm)	500	50	450	150
Bandgap (eV)	3.5	3.3	1.5	2.17
Electron Affinity (eV)	4.0	3.9	3.9	3.20
Dielectric permittivity (relative)	9.0	9.0	6.50	7.11
CB effective density of State ($\frac{1}{cm^3}$)	2.2×10^{17}	2×10^{17}	2.2×10^{18}	2.02×10^{17}
VB effective density of State ($\frac{1}{cm^3}$)	2.2×10^{16}	1×10^{17}	2.2×10^{18}	1.1×10^{19}
Electron thermal velocity ($^{cm}/_{s}$)	1×10^{7}	1×10^{7}	1×10^{7}	1×10^{7}
Hole thermal velocity ($^{cm}/_{s}$)	1×10^{7}	1×10^{7}	1×10^{7}	1×10^{7}
Electron Mobility ($\frac{cm^2}{vs}$)	20	20	2	200
hole Mobility ($\frac{cm^2}{vs}$)	10	10	2	80
Shallow ND ($\frac{1}{cm^3}$)	1×10^{15}	6×10^{18}	0	0
Shallow NA ($\frac{1}{cm^3}$)	0	0	1×10^{13}	6×10^{18}
Defect density (Nt)			2.5×10^{13}	

Table 2: Optimized Parameter for simulation of the proposed perovskite solar Cells

Parameters	FTO(SnO_2)	TiO_2 (ETL)	MAPbI3	CU_2O (HTL)
Thickness (nm)	500	50	1200	200
Bandgap (eV)	3.5	1.2	1.40	1.9
Electron Affinity (eV)	4.0	3.9	3.9	3.20
Dielectric permittivity (relative)	9.0	9.0	6.50	7.11
CB effective density of State ($\frac{1}{cm^3}$)	2.2×10^{17}	2×10^{17}	2.2×10^{18}	2.02×10^{17}

VB effective density of State ($\frac{1}{cm^3}$)	2.2×10^{16}	1×10^{17}	2.2×10^{18}	1.1×10^{19}
Electron thermal velocity $(^{cm}/_{s})$	1×10^{7}	1×10^{7}	1×10^{7}	1×10^{7}
Hole thermal velocity $(^{cm}/_{s})$	1×10^{7}	1×10^{7}	1×10^{7}	1×10^{7}
Electron Mobility $(\frac{cm^2}{vs})$	20	20	2	200
Hole Mobility $(\frac{cm^2}{vs})$	10	10	2	80
Shallow ND ($\frac{1}{cm^3}$)	1×10^{15}	6×10^{18}	0	0
Shollow NA ($\frac{1}{cm^3}$)	0	0	1×10^{13}	6×10^{18}
Defect density (Nt)			1.0×10^{8}	

Result and Discussion

In this work, the numerical study was performed on lead-based organic-inorganic perovskite to enhance its performance, minimize the toxicity, and stabilize the PSCs. To do this, the experimental parameters of the PSCs were obtained from existing work as shown in Table 1 and the SCAPS -1D simulator was used to simulate results for the initial call as shown in Figure 1. The result of our work revealed that the short-circuit current density (Jsc) was 24.80 mA/ cm^2, the open-circuit voltage (Voc) was 1.28 V, the power conversion efficiency (PCE) of 16.73%, and the fill factor (% FF) of 84.49% recorded. We slightly altered some parameters as shown in the proposed (Figure 1 b) and repeated the simulation to ascertain the influence of the proposed device's thickness, bandgap, defect density, and temperature.

Influence of Thickness on the Device HTL

The thickness of the proposed device was varied from 0.2 μm to 1.2 μm to observe its influence on the hole transport layer. The results of this variation are shown in Table 3 and it shows that the power conversion efficiency increases as the thickness of the device increases from 0. 2 μm to 1.0 μm but decreases at further increases in thickness. The higher PCE value observed at the 1.0 μm thickness agreed with [24] as they reported that perovskite layer thickness is important for high-performing devices and there is no advantage to using thinner (<200 nm) or thicker (>700 nm) film in the device.

The device fill factor and open-circuit voltage did not show any significant difference as we varied thickness. This shows that the proposed device is insensitive to the device's thickness as already reported by Dutta and Chatterjee [25, 26]. However, a higher FF of more than 80% is necessary for high-performing perovskite solar cells [26]. The short-circuit current density (Jsc) of the device increases slightly as the thickness increases and can likely mean that the device absorbs photons. This behaviour is consistent with the conclusion credited to Sikiru et al. who said when the short-circuit current density increases as the thickness of a material increases, it means that the material is more likely to absorb photons [27] and this Jsc can also improve the quantum efficiency of a solar cell.

The effects of thickness of the device on the HTL are illustrated in Figure 1. The correlation between the PCE and FF is shown in Figure 2 (a), Figure 2 (b) is shown behaviour of the Jsc and Voc with respect to varied thickness of the HTL, and Figure 2 (c) relates the current density and the voltage at varying thickness.

Table 3: J-V characteristic parameters with the variation of thickness of the HTM

Thickness (nm)	**PCE (%)**	**FF (%)**	**J_{sc}(mAcm^{-2})**	**V_{oc} (V)**
0.2	26.76	84.89	24.83	1.28
0.4	26.83	84.89	24.89	1.28
0.6	26.86	84.89	24.92	1.28
0.8	26.88	84.89	24.94	1.28
1.0	26.89	84.89	24.95	1.28
1.2	26.71	84.89	24.96	1.28

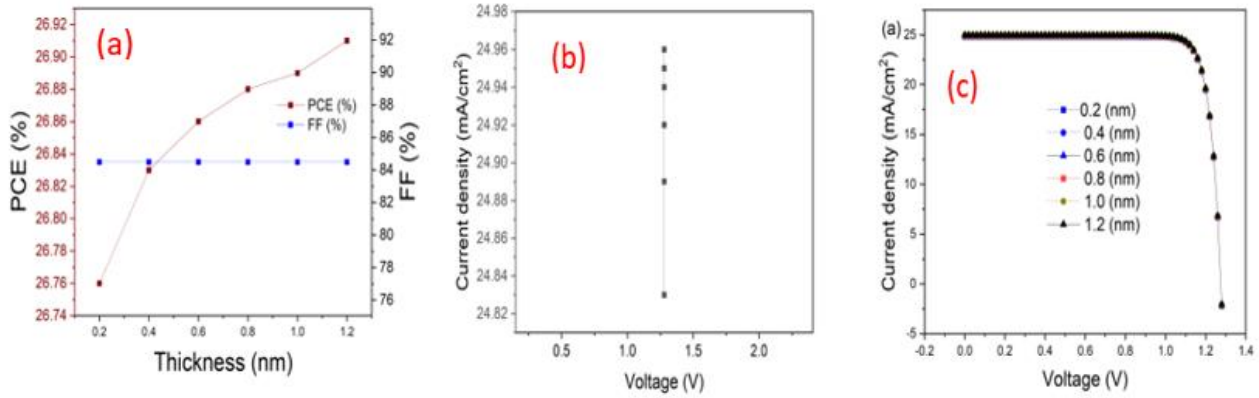

Figure 2**.** (a) PCE and FF concerning the thickness of the HTL, (b) Jsc and Voc concerning the varied thickness of the HTL, and (c) J-V curve with varied HTL thickness.

Influence of Thickness on the Device Absorber Layer

The thickness of the absorber layer also varied from 0.2 µm to 1.2 µm and we witnessed an increase in the PCE as the thickness increased except 1.2 µm. This increase in the (PCE) of the perovskite solar cell as the thickness of the absorber layer increases is consistent with those reported in the works of literature [28, 29, 30]. The 1.0 µm thickness recorded the highest (PCE) which in this work, is the optimum value. The FF, the J_{sc}, and V_{oc} also increased as the thickness of the absorber layer increased. However, there is a limit to how thick the layer can be, and increasing it beyond a 1.0 µm can decrease the cell's performance (see Table 4). But as the thickness of the absorbing layer increases, it enhances light absorption, leading to an increase in Jsc [29].

The current density has been plotted against the thickness as shown in Figure 3 (a) and the correction between the PCE and FF is shown in Figure 3 (b). These Figures are in complete agreement with the work carried out by [29] as the Jsc enhances the performance of the PSCs.

Table 4: J-V characteristic parameters with the variation of thickness of the absorber layer

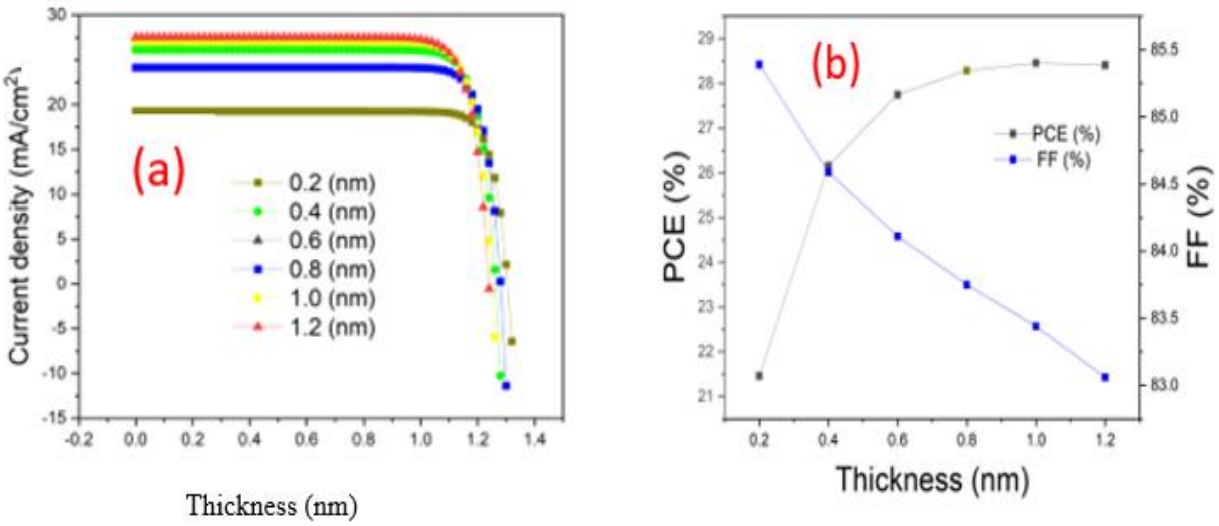

Figure 3: (a) J-V curve with varied absorber and (b) PCE and FF concerning the thickness of the absorber layer

The Effect of Temperature on the Perovskite Device.

Thermal instability has been reported as one major obstacle hindering the commercialization of perovskite solar cells [31, 32]. The temperature effect on mesoporous triple-cation perovskite solar cells with two different hole extraction materials has been investigated [33]. They observed that at low temperatures, the devices present very stable values (average loss <5 %), but as the temperature

Thickness (nm)	**PCE (%)**	**FF (%)**	**J_{sc}(mAcm^{-2})**	**V_{oc} (V)**
0.2	21.46	85.39	19.26	1.31
0.4	26.16	84.59	24.15	1.28
0.6	27.75	84.11	26.12	1.26
0.8	28.29	83.75	27.04	1.25
1.0	28.46	83.44	27.53	1.24
1.2	28.41	83.06	27.81	1.23

increases significant decreases in the open circuit potential and short-circuit current were witnessed. In this work, a working temperature of 300k was used to simulate the initial structure cell as shown in Figure 1 (a) and thereafter the temperature was varied from 280k to 340k. This variation in the

working temperature of the PSCs was done to obtain the best-performing temperature. The result of our simulation revealed that the PSC perform better at lower temperatures as shown in Figure 4 (a). This behaviour is similar to the one reported by [33] and this showed the PSCs are more stable at lower temperatures. The correlation between the PCE and FF at different temperatures is shown in Figure 4 (b) and our results revealed high FF at lower temperatures. These temperatures correspond with the higher PCE but decrease as the FF increases.

Table 5: J-V characteristic parameters with the variation of Temperature of the perovskite device.

Temperature (K)	**PCE (%)**	**FF (%)**	**J_{sc}(mAcm^{-2})**	**V_{oc} (V)**
280	27.46	85.36	24.80	1.29
290	27.06	84.90	24.80	1.28
300	26.73	84.49	24.80	1.27
310	26.35	84.00	24.81	1.26
320	25.97	83.50	24.81	1.25
330	25.61	83.09	24.81	1.24
340	25.23	82.61	24.81	1.23

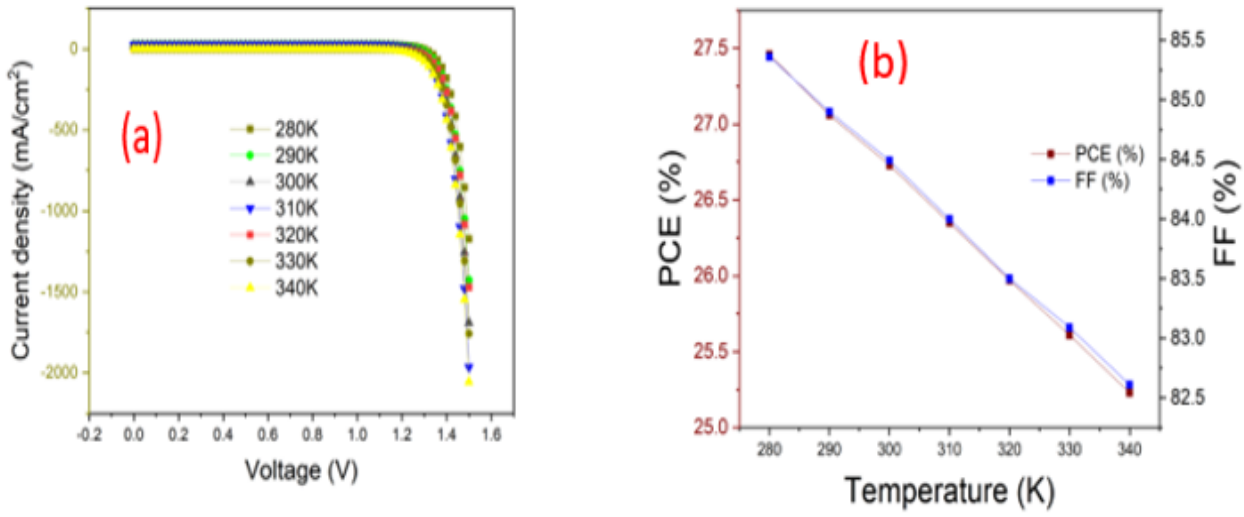

Figure 4*.* *(a)* J-V curve with varied Temperature. (b) the correlation between PCE and FF

Effect of Interface Defect Density on the Perovskite Solar Sell (PSC)

In this work, the interface defect density at HTL interface of the proposed solar cell architecture varied from 10^8 cm^{-2} to 10^{13} cm^{-2} . The other parameters were kept constant throughout the simulation and the result revealed that the PCE decreases as the device interface defect density increases Table 6. The device's high efficiency of 28.50% was obtained at a defect density of 10^8 cm^{-2}. The device FF, J_{sc} and V_{oc} also decrease as the interface defect density increases. The decline in the J_{sc} and V_{oc} is attributed to the instant generation of abundant recombination sites in the HTL and interfaces [34]. The decrease in the fill factor (FF) as the HTL interface defect density in the perovskite solar cell increases is due to the increase in the recombination centers and series resistance [35].

Table 6: J-V characteristic parameters with the variation of ETL/absorber interface defect density of the perovskite device.

Nt (cm^{-2})	PCE (%)	FF (%)	J_{sc}($mAcm^{-2}$)	V_{oc} (V)
10^8	28.50	85.56	24.81	1.47
10^9	28.22	84.50	24.80	1.45

10^{10}	28.16	84.00	24.78	1.44
10^{11}	27.56	83.50	24.75	1.42
10^{12}	26.31	83.00	23.81	1.38
10^{13}	21.71	79.52	23.76	1.32

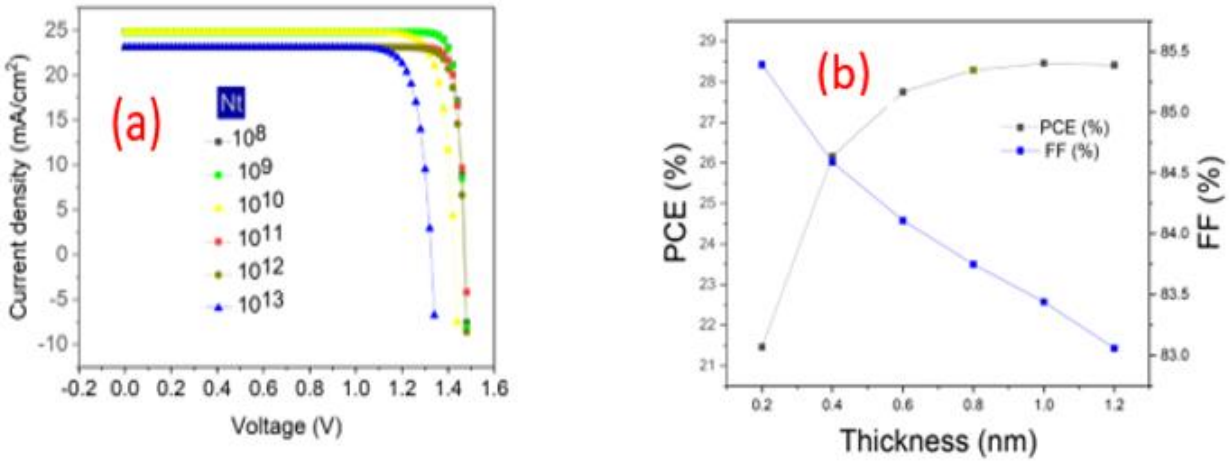

Figure 5. *(a) J-V curve with varied interface defect density. (b) PCE and FF with respect to interface defect density*

Influence of Bandgap on the Device ETL

The bandgap of a perovskite solar cell (PSC) affects the optoelectronic characteristics of the material and the variation in the bandgap can impact the hole transport layer (HTL) in different ways. In this work, the bandgap of the PSC was varied from 1.2 eV to 1.7 eV as shown in Table 7. The result shows the high performance of the device at the low bandgap but the PCE, FF, J_{sc}, and V_{oc} decrease as the bandgap increases. The low bandgap of the perovskite material indicates that the PSCs degrade more quickly than the high bandgap [36, 37]. The bandgap of a perovskite solar cell also has a significant effect on its short-circuit density (Jsc), open-circuit voltage (Voc), and fill factor (FF) as shown in Figure 6. The decrease in the Jsc as the bandgap increases is because the Jsc is related to the absorption of light. The lower bandgaps usually allow perovskite materials to absorb more of the

solar spectrum. This behaviour is in agreement with the work done by Mortadi el al. [38]. However, the open-circuit voltage and the fill factor increase with increasing bandgap which is contrary to the result reported by [38].

Table 7: J-V characteristic parameters with the variation of bandgap of the ETL.

Bandgap (eV)	PCE (%)	FF (%)	J_{sc}(mAcm^{-2})	V_{oc} (V)
1.2	29.13	86.73	27.14	1.33
1.3	28.67	84.66	26.54	1.28
1.4	27.91	84.48	25.86	1.28
1.5	27.32	84.48	25.33	1.28
1.6	27.08	84.48	25.12	1.28
1.7	26.08	84.48	25.00	1.28

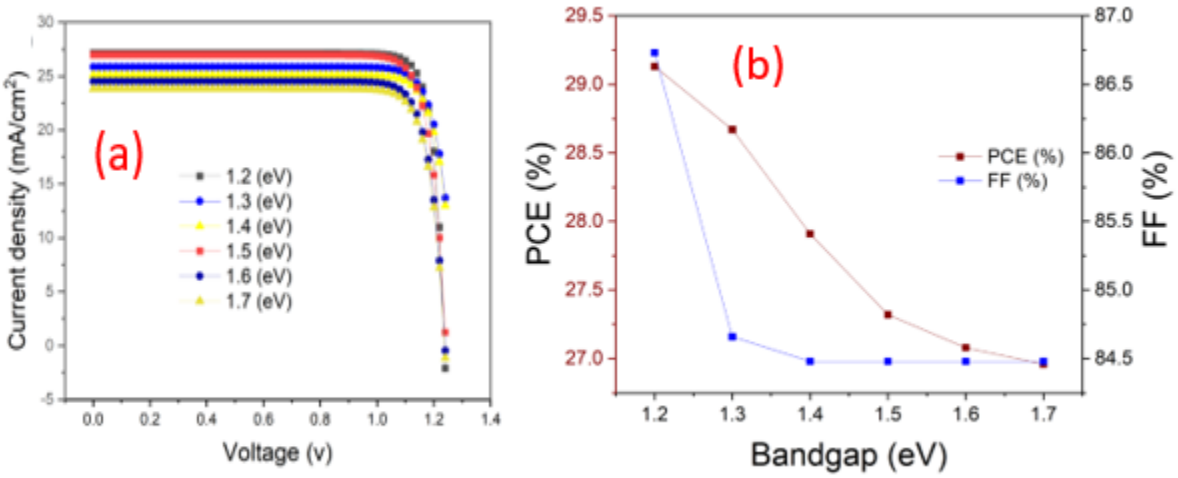

Figure 6. *(a) J-V curve with varied ETL Bandgap. (b) PCE and FF with respect to Bandgap of the ETL*

Influence of Bandgap on the Device HTL

The bandgap was varied from 1.8 eV to 2.3 eV in the HTL because lower bandgaps were showing convergence failure. The result of varying bandgap on the device hole transport layer (HTL) is consistent with [38] as the Jsc decreases with an increase in the bandgap and the Voc and FF both increase with increasing bandgap. This is because the Voc is related to the energy level alignment of

the solar cell. The larger bandgaps usually allow perovskite materials to generate a large thermal voltage [38, 39]. The FF which is the measure of how the solar cell converts sunlight into electricity efficiently is consistent with the result obtained by Mortadi el al. [38].

Table 8: J-V characteristic parameters with the variation of bandgap of the HTM

Bandgap **(ev)**	**PCE (%)**	**FF (%)**	**J_{sc}(mAcm^{-2})**	**V_{oc} (V)**
1.8	26.49	82.71	24.08	1.24
1.9	26.68	84.01	24.97	1.25
2.0	26.64	83.89	25.43	1.27
2.1	26.70	84.35	25.64	1.28
2.2	26.73	84.50	25.79	1.29
2.3	26.72	84.50	25.76	1.30

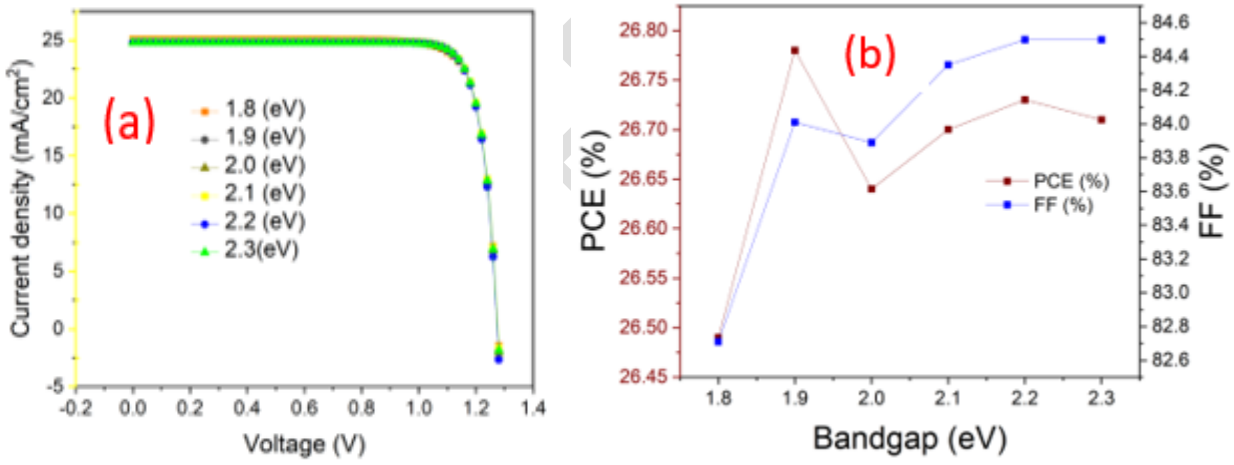

Figure 7. *(a) J-V curve with varied HTL bandgap and (b) PCE and FF with respect to bandgap of HTL*

Influence of Bandgap on the absorber layer

It was observed that the J-V curve shown in Figure 8 after varying the bandgap ranging from 1.40 to 1.65eV of the absorber layer, there is a decrease in short circuit current density (Jsc) at 28.45mA/cm2 but increases in open circuit voltage (Voc) at 1.18V, FF at 83.42% and PCE at 28.08% which are the optimized parameters for the bandgap due to increase of photoconductivity and photosensitivity.

Furthermore, at 1.65eV, Jsc at 20.15mA/cm2 and PCE at 24.26% decrease due to the increase of Voc at 1.41V and FF at 85.03% because of the decrease of photoconductivity and photosensitivity.

Table 9: J-V characteristic parameters with the variation of bandgap of the absorber layer.

Bandgap (eV)	**PCE (%)**	**FF (%)**	**J_{sc}(mAcm^{-2})**	**V_{oc} (V)**
1.40	28.08	83.42	28.45	1.18
1.45	27.30	83.99	26.43	1.23
1.50	26.70	84.49	24.80	1.28
1.55	25.84	84.87	23.04	1.32
1.60	25.21	85.03	21.67	1.37
1.65	24.26	85.03	20.15	1.41

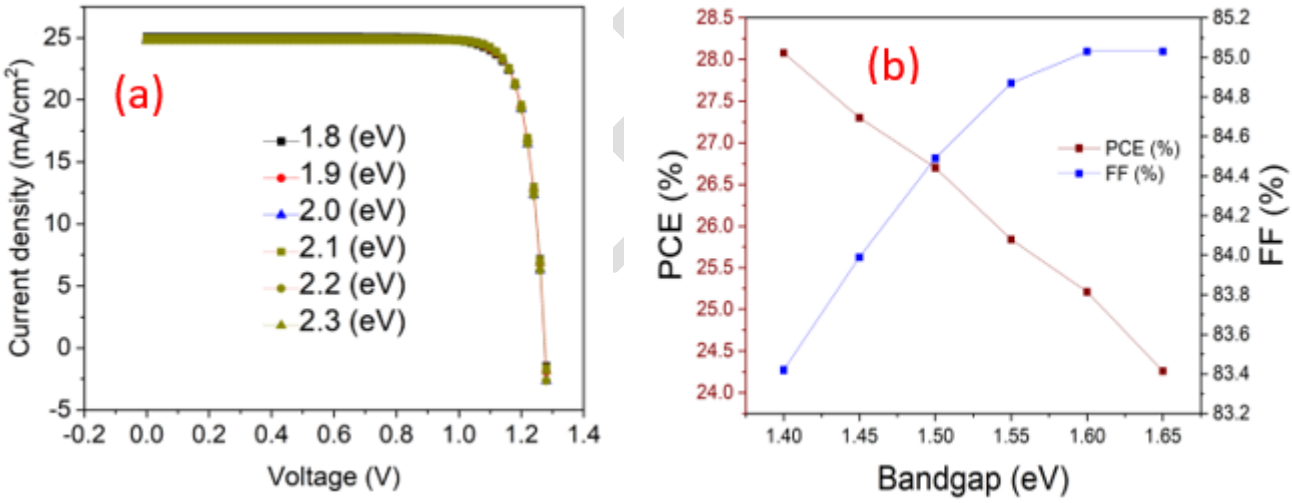

Figure 8. *(a) J-V curve with varied absorber Bandgap. (b) PCE and FF with respect to Bandgap of the absorber layer*

Conclusion

In this paper, a numerical simulation of a normal n-i-p planar PSC having the configuration of FTO/TiO_2/$MAPbI_3$/Cu_2O/Pt is performed using the SCAPS-1D simulation software. We used TiO_2 ETM due to its higher charge mobility. We first calculated/extracted the absorption coefficient of all the

layers and inserted them as input data in the SCAPS1-D software. Then, we carried out the simulations. Several factors that affect the cell's performance have been investigated. These factors include $MAPbI_3$ layer thickness, the absorber defect density, Bandgap and the operating temperature. We found that all these factors influence the electrical parameters of PSC. The results revealed that the optimal $MAPbI_3$ thickness was 1.0 μm. Also, the optimum value of the absorber defect density $10^8 cm^2$ bandgap 1.40eV, and the operating temperature is 280 K.

REFERENCES

[1]. G. Dastgeer, M. Imran, S. Nisar, K. Akbar, & M. Wajid. A review on recent progress and challenges in high-efficiency perovskite solar cells, *Nano Energy*, 132 (2024) 110401

[2]. T. Ibn-Mohammed, S.C.L. Koha, I.M. Reaney, A. Acquaye, G. Schileo, K.B. Mustapha, & R. Greenough. Perovskite solar cells: An integrated hybrid lifecycle assessment and review in comparison with other photovoltaic technologies, *Renewable and Sustainable Energy Reviews*, 80 (2017) 1321 - 1344

[3]. F. Alharbi, I. Hossain, & N. Tabet. Perovskite based solar cells: A milestone towards cheaper PV technology, Conference: The 3rd Int'l Symp. on Environment-Friendly Energies and Applications, EFEA, (2014), At: Paris, France

[4]. R. Wang, M. Mujahid, Y. Duan, Z. Wang, J. Xue, & Y. Yang. A Review of Perovskites Solar Cell Stability, *Adv. Funct. Mater*. (2019) 1808843

[5]. H. J. Kim, G.S. Han and H. S. Jung. Managing the lifecycle of perovskite solar cells: Addressing stability and environmental concerns from utilization to end-of-life, *eScience* 4 (2024) 100243

[6]. U. Erdil, M. Khenkin, W. M. Bernardes de Araujo, Q. Emery, I. Lauermann, R. Schlatmann, A. Abate, & C. Ulbrich. Delamination of Perovskite Solar Cells in Thermal Cycling and Outdoor Tests, Energy *Technol*. (2024) 2401280

[7]. G. Abdelmageed, C. Mackeen, K. Hellier, L. Jewel, L. Seymour, M. Tingwald, F. Bridges, J. Z. Zhang, & S. Carter. Effect of temperature on light-induced degradation in methylammonium lead iodide perovskite thin films and solar cells, *Solar Energy Mater. & Solar Cell*s 174 (2018) 566 -571

[8]. T.T. Ava, A. Al Mamun, S. Marsillac, and G. Namkoong. A Review: Thermal Stability of Methylammonium Lead Halide-Based Perovskite Solar Cells, *Appl. Sci*. (2019) 9, 188

[9]. H.S. Kim, J.W. Lee, N. Yantara, P.P. Boix, S.A. Kulkarni, S. Mhaisalkar, M. Grätzel, & N. G. Park. High efficiency solid-state sensitized solar cell-based on submicrometer rutile TiO_2 nanorod and $CH_3NH_3PbI_3$ perovskite sensitizer. *Nano Letters*, (2013) *13*(6), 2412-2417

[10]. X. Shen, K. Kang, Z. Yu, W. H. Jeong, H. Choi, S. H. Park, S. D. Stranks, H. J. Snaith, R. H. Friend, & B. R. Lee. Passivation strategies for mitigating defect challenges in halide perovskite light-emitting diodes, *Joule* 7, (2023), 272–308

[11]. G. G. Njema, J. K. Kibet, & S. M. Ngari. A review of interface engineering characteristics for high-performance perovskite solar cells, *Measurement: Energy* 2 (2024) 100005

[12]. S. AL-Shujaa, P. Zhao, D. He, B. Al-Anesi, Y. Feng, J. Xia, B. Zhang, & Y. Zhang. Improving the Efficiency and Stability of Perovskite Solar Cells by Refining the Perovskite-Electron Transport Layer Interface and Shielding the Absorber from UV Effects, *ACS Appl. Mater. Interface*, 16 (2024), 28494 – 28504

[13]. C. Yang, W. Hu, J. Liu, C. Han, Q. Gao, A. Mei, Y. Zhou, F. Guo, & H. Han. Achievements, challenges, and future prospects for industrialization of perovskite solar cells, *Light: Science & Applications* (2024) 13:227

[14]. Z. Ni, H. Jiao, C. Fei, H. Gu, S. Xu, Z. Yu, G. Yang, Y. Deng, Q. Jiang, Y. Liu, Y. Yan, & J. Huang. Evolution of defects during the degradation of metal halide perovskite solar cells under reverse bias and illumination, *Nature Energy*, 7 (2022), 65 -73.

[15]. S. Zandi, P. Saxena, & N. Gorji. Numerical simulation of heat distribution in RGO-contacted perovskite solar cells using COMSOL, *Solar Energy*, 197 (2020), 105 – 110

[16]. S. Michael, A.D. Bates, & M.S. Green. Silvaco ATLAS as a solar cell modeling tool, Conference: Photovoltaic Specialists Conference, (2005). Conference Record of the Thirty-first IEEE

[17]. O. Ahmad, I. Qasim, S. M. Hasnain, Z. ul Abdin, M. F. Nasir, M. I. Malik, & A. Rashid. Modelling and numerical simulations of eco-friendly double absorber solar cell "Spiro-Ome TAD/CIGS/$MASnI_3$/CdS/ZnO" and its PV-module, *Organic Electronics* 117 (2023) 106781

[18]. E. Danladi, P.M. Gyuk, N.N. Tasie, A.C. Egbugha, D. Behera, I. Hossain, M. Bagudo, M.L. Madugu, J.T. Ikyumbur**.** Impact of hole transport material on perovskite solar cells with different metal electrode: A SCAPS-1D simulation insight, *Heliyon* 9(6) (2023) https://doi.org/10.1016/j.heliyon,2023e16838

[19]. J.T. Ikyumbur, F. Gbaorun, A.A. McAsule, T.M. Aper, N.S. Akiiga, A.A. Gundu, M.S. ShiadaSCAPS-1D simulation of a high-efficiency quantum dot solar cell using Sb_2Se_3 as an absorber layer, *Next Research* **1** (2024)**,** 100084

[20]. J. A. Ukwenya, J. A. Owolabi, M.Y. Onimisi, E. Danladi, S. M. Udeh, & U. R. Ushiekpan. The Effect of Temperature Dependence on Tin Perovskite Solar Cell using SCAPS 1D, FUDMA *Journal of Sciences* 7(2) (2023) 321 – 329

[21]. U. Mandadapu, S. V. Vedanayakam & K. Thyagarajan. Simulation and Analysis of Lead based Perovskite Solar Cell using SCAPS-1D, *Indian Journal of Science and Technology*, 10(11) (2017)

[22]. A.M. Abena, A. Ntouga, T. Ngoupo, A. Abega, J.M.B. Ndjaka. Numerical investigation of solar cells based on hybrid organic cation perovskite with inorganic HTL via SCAPS-1D, *Chinese J. Phys.*, 76 (2022), 94-109

[23]. A. Hajjiah, M. Gamal, I. Kandas, N. E. Gorji, N. ShehataDFT and AMPS-1D simulation analysis of all-perovskite solar cells based on CsPbI3/FAPbI3 bilayer structure, *Sol. Energy Maters. and Sol. Cells,* 248 **(**2022) 112026

[24]. A. Bag, R. Radhakrishnan, R. Nekovei, & R. Jeyakumar. Effect of absorber layer, hole transport layer thicknesses, and its doping density on the performance of perovskite solar cells by device simulation, *Sol. Energy*, 196 (2020), 177 – 182

[25]. U. Dutta & P. Chatterjee. The open circuit voltage in amorphous silicon p-i-n solar cells and its relationship to material, device and dark diode parameters, *J. Appl. Phys.*96 (4) (2004), 2261-2271

[26]. X. Zhang, C. Li, J. Xu, R. Wang, J. Song, H. Zhang, Y. Li, Y. Jing, S. Li, G. Wu, J. Zhou, X. Li, Y. Zhang, X. Li, J. Zhang, C. Zhang, H. Zhou, Y. Sun, & Y. Zhang. High fill factor organic solar cells with increased dielectric constant and molecular packing density, *Joule* 6 (2022),444–457

[27]. S. Sikiru, T. L. Oladosu, T. I. Amosa, S. Y. Kolawole, & H. Soleimani. Recent advances and impact of phase change materials on solar energy: A comprehensive review, *J. Energy Storage*, 53 (2022) 105200

[28]. A. Mortadi, E. El Hafidi, M. Monkade, & R. El Moznine. Investigating the influence of absorber layer thickness on the performance of perovskite solar cells: A combined simulation and impedance spectroscopy study, *Mater. Sc. Energy Tech.*, 7 (2024) 158- 165

[29]. A. H. Oishi, Md T. Anjum, Md M. Islam, & Md F. Nayan. Impact of Absorber Layer Thickness on Perovskite Solar Cell Efficiency: A Performance Analysis, *EJECE*, (2023), 7(2):48-51

[30]. S. Imani, S. M. Seyed-Talebi, J. Beheshtian, & E.W. G. Diau. Simulation and characterization of CH3NH3SnI3-based perovskite solar cells with different Cu-based hole transporting layers, *Appl. Phys.* A (2023) 129:143

[31]. H. Zheng, G. Liu, C. Zhang, L. Zhu, A. Alsaedi, T. Hayat, X. Pan, & S. Dai. The influence of perovskite layer and hole transport material on the temperature stability about perovskite solar cells, *Sol. Energy* 159 (2018) 914-919

[32]. L. Zhang, Y. Wang, X. Meng, J. Zhang, P. Wu, M. Wang, F. Cao, C. Chen, Z. Wang, F. Yang, X. Li, Y. Zou, X. Jin, Y. Jiang, H. Li, Y. Liu, T. Bu, B. Yan, Y. Li, J. Fang, L. Xia, J. Yang, F. Huang, S. Liu, J. Yao, L. Liao, L. Li, F. Zhang, Y. Zhan, Y. Chen, Y. Mai, & L. Ding. The issues on the commercialization of perovskite solar cells, *Mater. Futures* 3 (2024) 022101

[33]. I. Mesquita, L. Andrade, & A. Mendes. Temperature Impact on Perovskite Solar Cells Under Operation, *Energy Mater.*, (2019), 12 (10), 2186-2194

[34]. F. Anwar, R. Mahbub, S.S. Satter, & S.M. Ullah. Effect of Different HTM Layers and Electrical Parameters on ZnO Nanorod-Based Lead-Free Perovskite Solar Cell for High-Efficiency Performance. *Int. J. Photoenergy* (2017) 9846310.

[35]. A. S. Chouhan, N. P. Jasti, & S. Avasthi. Effect of Interface Defect Density on Performance of Perovskite Solar Cell: Correlation of Simulation and Experiment, *Mater. Lett.* 221 (2018), 150 - 153

[36]. Y. Kawano, J. Chantana, T. Negami, T. Nishimura, A. Mavlonov, & T. Minemoto. Theoretical impacts of single band gap grading of perovskite and valence band offset of perovskite/hole transport layer interface on its solar cell performances, *Sol. Energy,* 231 (2022) 684 -693

[37]. M. Ahamad & A.K.M. A. Hossain. Design and optimization of non-toxic and highly efficient tin-based organic perovskite solar cells by device simulation, *Hellyon*, 9 (2023) e19389

[38]. A. Mortadi, El M. El Hafidi, H. Nasrellah, M. Monkade, & R. El Moznine. Investigation of bandgap grading on performances of perovskite solar cell using SCAPS-1D and impedance spectroscopy, *Sol. Energy Advans.* 4 (2024) 100056

[39]. T. C. Yang, P. Fiala, Q. Jeangros, & C. Ballif. High-Bandgap Perovskite Materials for Multijunction Solar Cells, *Joule,* 2(8) (2018) 1421-1436.